

Three Different Behaviors of Liquid Water Path of Water Clouds in Aerosol-Cloud Interactions

Qingyuan Han¹, William B. Rossow², Jian Zeng¹, and Ronald Welch¹

¹ University of Alabama in Huntsville
Huntsville, AL

²NASA/Goddard Institute for Space Studies
New York, NY

Abstract

Estimates of the indirect aerosol effect in GCMs assume either that cloud liquid water path is constant (Twomey effect) or increases with increased droplet number concentration (drizzle-suppression or Albrecht effect). On the other hand, if cloud thermodynamics and dynamics are considered, cloud liquid water path may also decrease with increasing droplet number concentration, which has been predicted by model calculations and observed in ship-track and urban influence studies. This study examines the different changes of cloud liquid water path associated with changes of cloud droplet number concentration. Satellite data (January, April, July and October 1987) are used to determine the cloud liquid water sensitivity, defined as the ratio of changes of liquid water path and changes of column droplet number concentration. The results of a global survey for water clouds (cloud top temperature $>273\text{K}$, optical thickness $1 \leq \tau < 15$) reveal all three behaviors of cloud liquid water path with aerosol changes: increasing, approximately constant, or decreasing as cloud column number concentration increases. We find that (1) in about one third of the cases, predominantly in warmer locations or seasons, the cloud liquid water sensitivity is negative and the regional and seasonal variations of the negative liquid water sensitivity are consistent with other observations, (2) in about one third of the cases, a minus one third ($-1/3$) power law relation between effective droplet radius and column number concentration is found, consistent with a nearly constant cloud water path, and (3) in the remaining one third of the cases, the cloud liquid water sensitivity is positive. These results support the suggestion that it is possible for an increase of cloud droplet number concentration to both reduce cloud droplet size and enhance evaporation just below cloud base, which decouples the cloud from the boundary layer in warmer locations, decreasing water supply from surface and reducing cloud liquid water. Our results also suggest that the current evaluations of the negative aerosol indirect forcing by GCMs, which are based on either the Twomey or Albrecht effects, may be overestimated in magnitude.

1. Introduction

Aerosol radiative forcings, both direct and indirect, are the most uncertain atmospheric forcings of climate change. Between them, the aerosol indirect forcing, which is related to the cloud radiative property changes through cloud-aerosol interactions, is the most uncertain (IPCC 1996). The importance of the aerosol indirect effect is increased by the suggestion that it is the most likely explanation for the observed decrease of the diurnal temperature cycle (Hansen et al., 1997).

Significant progress has been made in recent years

to evaluate the aerosol indirect effect by using prognostic equations for liquid water content and cloud droplet number concentration in global climate models (e.g., Del Genio et al., 1996; Lohmann et al., 1999; Rotstayn, 1999; Ghan et al., 2001; Menon et al., 2000). These physically-based GCMs are more reliable in predicting changes in climate because they are not tuned to parameterizations that may only be valid under current climate conditions. However, the results of these models are quite different because cloud droplet number concentrations and cloud liquid water contents are calculated differently. To reduce the differences in global model results, and thus the uncertainties in estimations of the aerosol indirect effect, global satellite observations of cloud and aerosol properties and their relationships are crucially needed.

During the first phase of GACP (Global Aerosol Climatology Project), new variables and their relationships have been retrieved from satellite

*Corresponding author address: Dr. Qingyuan Han,
University of Alabama in Huntsville, 320 Sparkman
Drive, Huntsville, AL 35805.
E-mail: han@nsstc.uah.edu*

observations including near-global surveys of the relationship between cloud albedo and effective radius (Han et al., 1998a), cloud column number concentration (Han et al., 1998b), and cloud column susceptibility (Han et al. 2000). Some of these results have been used for comparisons with model predictions. For example, in the study reported by Han et al. (1998a), results of a near-global survey reveal that cloud albedo and droplet radius are positively correlated for most optically thin clouds ($\tau < 15$) and negatively correlated for most optically thick clouds ($\tau > 15$), where τ is referred to $\lambda = 0.6 \mu\text{m}$. Such a relationship compares favorably with the behavior exhibited by several GCMs (e.g., Lohmann et al., 1999; Ghan et al., 2001). Nevertheless, the estimated aerosol indirect effect (-1.7 W/m^2) from the MIRAGE model (Ghan et al., 2001) is much larger than that (-0.4 W/m^2) estimated by Lohmann et al. (1999) using the ECHAM model, even though the cloud liquid water content changes due to the aerosol effect are smaller in the MIRAGE than in the ECHAM model. This indicates that more detailed quantitative comparisons including relationships among different parameters and their variations are needed.

Cloud microphysics schemes in most GCMs include at least two variables: cloud droplet number concentration and cloud liquid water content (e.g., Del Genio et al., 1996; Lohmann et al., 1999; Ghan et al., 1997; Rotstayn, 1999; Menon et al., 2002) with droplet size inferred from these two. Increases in cloud droplet number concentration, N , are a direct indication of the aerosol-cloud interaction, considered the driving force of the indirect effect. This has been suggested by observations during the past several decades (e.g., Warner and Twomey, 1967; Fitzgerald and Spyers-Duran, 1973; Egan et al., 1974; Alkezweeny et al., 1993; Hudson and Svensson, 1995). The cloud liquid water content is the basic parameter for calculating cloud processes, especially radiation and precipitation. Therefore, model estimates of the aerosol indirect effect includes two links: one is to model the relation between cloud droplet number concentration and aerosol concentrations (e.g., Hudson et al., 2000 and references therein) and the other is to predict the cloud liquid water content with changing cloud droplet number concentrations (e.g., Durkee et al., 2000 and references therein). Following earlier investigations (for a review, see Twomey, 1993), most studies have been focused on the first link, producing empirical relations between aerosol concentrations and cloud droplet number concentrations (e.g., Jones et al., 1994, 1999; Boucher and Lohmann, 1995; Jones and Slingo, 1996; Rotstayn, 1999) and physically-based aerosol activation relations (e.g., Ghan et al., 1997; Lohmann et al., 1999). The intention of this study is to

investigate the second link, i.e., to examine the changes of cloud liquid water associated with changes of cloud droplet number concentration.

Based on a consideration of cloud microphysics, Albrecht et al. (1989) proposed that increased droplet number concentration leads to smaller droplet sizes that make precipitation formation more difficult producing larger water contents. This idea is supported by observations showing increased liquid water path and suppressed drizzle in ship tracks (Radke et al., 1989; Ferek et al., 2000) and in smoke plumes (Rosenfeld et al., 1999). However, model studies with a more complete treatment of the interactions of cloud dynamics, thermodynamics and radiation show that, even though drizzle is suppressed, cooling just below cloud base is enhanced because the smaller (and more numerous) cloud droplets evaporate more rapidly. This cooling acts together with the radiative heating of the cloud base to suppress turbulent mixing, decoupling the cloud from the rest of the boundary layer and reducing the supply of water vapor and of the cloud liquid water. In particular, Ackerman et al. (1995) show that these changes increase the amplitude of the diurnal cycle of cloud water content because the Albrecht effect operates at night to increase cloud water content but that this is overwhelmed during the day because the evaporative cooling reinforces the tendency for the cloud layer to decouple from the rest of the boundary layer. Decreased liquid water contents with increased droplet number concentration are also supported by observations of ship tracks (e.g., Platnick et al., 2000, Ackerman et al., 2000) and of urban influences on cloud properties (Fitzgerald and Spyers-Duran, 1973).

In current GCMs, the response of cloud liquid water to changes in droplet number concentration is through the influence of droplet number on the autoconversion of cloud water to rain, i.e., larger droplet concentration will either decrease the autoconversion rate of cloud droplets (e.g., Beheng, 1994; Lohmann and Feichter, 1997) or increase the critical threshold for autoconversion to start (e.g., Rotstayn, 1999). These mechanisms lead to a general increase in cloud liquid water content with increasing droplet number (e.g., Ghan et al., 2001). Although evaporation and its influence on droplet sizes are considered in a few GCMs (e.g., Lohmann et al., 1999), its influence on thermodynamics and the feedback on cloud liquid water is difficult to parameterize partially due to the coarse vertical resolution in GCMs (Del Genio, 2000, personal communication).

The questions are: what is the general behavior of cloud liquid water in response to increased droplet number concentrations and what are its temporal and spatial variations? If cloud liquid water increases with increased droplet number in the majority of clouds, then the consideration of cloud microphysics is good enough

and we are confident about the responses of cloud liquid water (and thus cloud optical properties) to aerosol-cloud interactions. If this is not the case, then more effort has to be made to include the difficult but important effects of cloud dynamics and thermodynamics in models for an accurate estimation of the aerosol indirect effect.

The purpose of this study is to answer the above questions using satellite observations. The concept of the cloud liquid water sensitivity is defined in section 2. The satellite data used in this study are described in section 3. Results and conclusions are presented in section 4 and 5, respectively.

2. Cloud liquid water sensitivity

We start with a definition that makes the comparison between results of model prediction and satellite observation more precise. Since observations show that changes in cloud geometrical thickness during aerosol-cloud interactions cannot be ignored (e.g., Hobbs et al., 1970, Ackerman et al., 2000), consistent with model predictions (Pincus and Baker, 1994; Ackerman et al., 1993), column-integrated values of cloud droplet number concentration, N_c , and liquid water content, LWP , are more appropriate in describing this relationship to avoid assumptions of constant geometrical thickness of the clouds. Satellite remote sensing can provide estimates of these column-integrated parameters, i.e., column droplet number concentration (Han et al., 1998b),

$$N_c = N \cdot h \quad (1)$$

and liquid water path (e.g., Greenwald et al., 1995, Han et al., 1994)

$$LWP = lwc \cdot h \quad (2)$$

where h is the cloud geometrical thickness. The form of (1) and (2) assumes vertical uniformity; in the more general case the satellite retrieval represents the vertical integrals of N and LWC . The relation between LWP and N_c is (Han et al., 1998b)

$$N_c = \frac{3}{4\pi\rho_w} \frac{LWP}{r_e^3(1-b)(1-2b)}$$

where b is the effective variance in a gamma size distribution.

We define the cloud water sensitivity as

$$\delta = \frac{\Delta LWP}{\Delta N_c} \quad (3)$$

when cloud thickness h is a constant, $\delta = \Delta LWC / \Delta N$. Note that this definition is similar to the definition of “cloud column susceptibility” (Han et al. 2000), in which $\Delta\alpha$ (changes in cloud spherical albedo) is replaced by ΔLWP (changes in cloud liquid water path). The reason that we do not use the term “susceptibility” here is that it means “apt to” or “the potential to be affected by” and therefore is determined by properties of individual clouds as first proposed by Twomey (1991). However, aerosol-cloud interactions are not only determined by the properties of clouds and aerosols, they are also determined by the conditions of environment such as thickness of boundary layer (e.g., Durkee et al., 2000). This is the reason that ship tracks are not found in many clouds with high susceptibilities (e.g., Platnick and Twomey, 1994; Coakley et al., 2000).

In our approach, the cloud water sensitivity, δ , is derived using the least-squares linear regression to determine the slope of ΔLWP and ΔN_c for all water clouds within a $2.5^\circ \times 2.5^\circ$ grid box during each one month period. Therefore, the derived value describes “what actually happened”, which is determined not only by cloud processes, but also by the condition of environments. In this sense, the terminology “cloud column susceptibility” used in Han et al. (2000) is misleading: it should be modified to “cloud albedo sensitivity” when it was derived based on monthly data from a grid box.

Liquid water sensitivity represents the change of liquid water path correlated with changes in column droplet number concentration, which is affected by the total water availability: clouds in a moist environment (e.g., maritime) tend to have larger liquid water sensitivity than those in a dry environment (e.g., continental). To this end, we normalize the liquid water sensitivity for different environments to isolate better the effect of aerosol-cloud interaction; the relative cloud water sensitivity is defined

$$\beta = \frac{\Delta LWP / LWP}{\Delta N_c / N_c} \approx \frac{\Delta \ln(LWP)}{\Delta \ln(N_c)} \quad (4)$$

The changes in LWP are caused by two factors, i.e., changes in volumetric mean droplet radius (\bar{r}) and changes in the column number concentration (N_c):

$$d \ln(LWP) = 3d \ln(\bar{r}) + d \ln(N_c)$$

If the relation between effective radius and volume average radius is used (e.g., Martin et al., 1994),

$$kr_e^3 = \bar{r}^3 \quad (5)$$

then the expression becomes

$$d \ln(LWP) = 3d \ln(r_e) + d \ln(k) + d \ln(N_c) \quad (6)$$

It is clear that the effect of change in k is not independent from changes in LWP ; it is part of the effect of changes in \bar{r} and thus part of the changes in LWP . Therefore, by estimating changes in LWP , the effect of changes in k is already included.

One relationship closely related to the liquid water sensitivity that is often used in models (e.g., Del Genio et al., 1996) is the relation between effective droplet radius, r_e , and volume number concentration, N_c :

$$r_e \propto N_c^{1/3} \quad \text{or} \quad \frac{d(\ln r_e)}{d(\ln N_c)} = -\frac{1}{3}$$

based on some observations (e.g., Stephens, 1978). For this relation to be valid, the liquid water content, effective variance, and cloud thickness have to be independent of N_c . There are aircraft measurements that either agree with or violate the above important relation (e.g., Ackerman et al., 2000) and no global statistics available to verify it. Although it is difficult to directly verify this relation using current satellite data, it is possible to check the slightly different relation

$$r_e \propto N_c^\gamma \quad \text{or} \quad \frac{d(\ln r_e)}{d(\ln N_c)} = \gamma \quad (7)$$

This relation is useful for verifying model results because N_c is the product of other two model parameters: volume number concentration (N) and cloud thickness (h). In case of zero liquid water sensitivity and negligible changes in k , the value γ would be $-1/3$.

3. Method and Data

The data used are the near-global datasets of cloud properties including cloud optical thickness, effective radius, liquid water path and column number concentrations for January, April, July and October 1987 developed using ISCCP data (Han et al., 1994, Han et al., 1998b). The original ISCCP analysis separates cloudy and clear image pixels (area about $4 \times 1 \text{ km}^2$ sampled to a spacing of about 30 km) and retrieves cloud optical thickness and top temperature (T_c) from radiances measured by AVHRR at wavelengths of 0.54 - 0.80 μm (Channel 1) and 10.0 - 11.6 μm (Channel 4), assuming $r_e = 10 \mu\text{m}$. The analysis uses the NOAA

TIROS Operational Vertical Sounder (TOVS) products to specify atmospheric temperature, humidity and ozone abundance and also retrieves the surface temperature (T_s). The ISCCP analysis is extended by retrieving r_e from AVHRR radiances at wavelengths of 3.44 - 4.04 μm (Channel 3) and revising the values of τ to be consistent for clouds with $T_c \geq 273 \text{ K}$ (Han et al., 1994, 1995). Only liquid water clouds are considered in this study because 90% of the tropospheric aerosols are distributed below 3 km altitude (Griggs, 1983). Moreover, aerosol effects on ice clouds may be different than on liquid water clouds. The radiances are modeled as functions of illumination/viewing geometry by including the effects of Lambertian reflection/emission from the surface (the ocean reflectance is anisotropic, see Rossow et al., 1989), absorption/emission by H_2O , CO_2 , O_3 , O_2 , N_2O , CH_4 , and N_2 with the correlated k-distribution method (Lacis and Oinas 1991), Rayleigh scattering by the atmosphere and Mie scattering/absorption by horizontally homogeneous cloud layers using a 12-Gauss point doubling/adding method. The droplet size distribution is assumed to be the gamma-distribution. Error sources are discussed and validation studies are reported in Han et al. (1994, 1995). Note that the satellite-measured radiation is only sensitive to the droplet sizes in the topmost part of the clouds; therefore, the values of LWP obtained by this analysis may be biased if r_e at cloud top is systematically different from the vertically averaged value (Nakajima et al., 1991). For non-precipitating clouds ($LWP \leq 150 \text{ g/m}^2$), the results of this method agree well with ground based microwave radiometer measurements (Han et al., 1995). Lin and Rossow (1994, 1996) show excellent agreement of microwave (from SSM/I) determinations of LWP over the global ocean with those obtained from the ISCCP results, assuming 10 μm droplets. Greenwald et al. (1997) compare microwave retrievals of LWP from SSM/I and from GOES-8 over the Pacific Ocean and they found RMS differences between these two independent retrievals is as low as 0.030 kg m^{-2} for overcast scenes.

The two parameters used to derive liquid water sensitivity, LWP and N_c , are obtained from r_e and τ by (Han et al., 1995),

$$LWP = \frac{2}{3} r_e \tau \rho_w \quad (8)$$

and (Han et al., 1998b)

$$N_c = \frac{\tau}{2\pi r_e^2 (1-b)(1-2b)} \quad (9)$$

where b is effective variance of cloud droplet size distribution. The value of b is taken as 0.193 in the retrieval of N_c , equivalent to a k value in Eq. (6) 0.495, which is smaller than the range of 0.67 to 0.80 as suggested by Martin et al. (1994) in order to offset the

effect of overestimate of r_e by satellite retrievals (Han et al., 1998b).

All of the individual pixel values are collected for each $2.5^\circ \times 2.5^\circ$ map grid cell for each month, representing both spatial variations at scales $\sim 10 - 100$ km and daily variations over each month. Only clouds with cloud top temperature warmer than 273 K were used in this study. To reduce the possible effects of cloud fractional cloud cover on cloud droplet radius (Han et al., 1995), only pixels with cloud optical thickness larger than unity were included. Since thinner clouds are more apt to be influenced by the aerosol indirect effect, only results of clouds with $1 \leq \tau < 15$ are shown. Typically, about 100 samples per map grid cell per month are available; results are not reported if there are fewer than 10 samples. Confidence level of the regression results varies with different grid boxes. On average, correlation coefficient $r=0.159$ is significant at the 0.95 confidence level.

The liquid water sensitivity, δ , is derived by least squares linear regression between LWP and N_c values. The power γ in the power law relation of r_e and N_c , which is related to the relative liquid water sensitivity, β , by Eq. (5), is derived by least squares linear regression between $\ln(r_e)$ and $\ln(N_c)$.

4. Results

4.1 Liquid Water Sensitivity

Figure 1 is a near-global survey of the liquid water sensitivity in water clouds for January, April, July and October 1987. Considering the whole range and

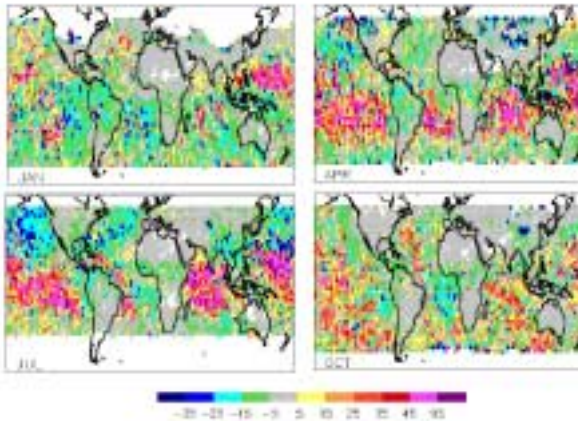


Figure 1: Liquid water sensitivity of water clouds for January, April, July and October 1987. The unit is in $[\text{g m}^{-2}/3 \times 10^6 \text{ cm}^{-2}]$. For a typical 300 m thickness of cloud, $1 [\text{g m}^{-2}/3 \times 10^6 \text{ cm}^{-2}]$ corresponds to an increase of cloud liquid water path by 1 g m^{-2} for a change of cloud droplet number concentration by 100 cm^{-3} .

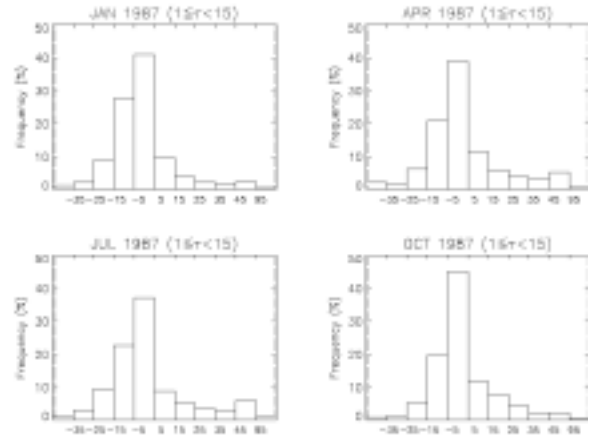


Figure 2: Histogram of the liquid water sensitivity for January, April, July and October 1987.

appropriate details in spatial variations, the units used are $[\text{g m}^{-2}/3 \times 10^6 \text{ cm}^{-2}]$. For a typical 300 m thickness of cloud (Wang et al., 2000), $1 [\text{g m}^{-2}/3 \times 10^6 \text{ cm}^{-2}]$ corresponds to an increase of cloud liquid water path by 1 g m^{-2} for a change of cloud droplet number concentration by 100 cm^{-3} . Green and blue colors represent negative liquid water sensitivities and yellow and red colors stand for positive liquid water sensitivities. The mean and standard deviations of the liquid water sensitivity are: -0.86 ± 19.6 , 3.95 ± 24.4 , 3.03 ± 25.8 , and 2.34 ± 16.7 for January, April, July and October 1987, respectively.

The most obvious feature is that negative liquid water sensitivities are by no means rare -- they are everywhere. For continental clouds, most clouds show neutral or slightly negative liquid water sensitivities. For maritime clouds, there are areas with both large negative and large positive liquid water sensitivities with a strong seasonal dependence, i.e., negative liquid water sensitivity is more common in the summer hemisphere. If the negative liquid water sensitivity is caused by decoupling of boundary layer, then the above relation suggests that the decoupling happens more often in warm areas than cold areas. This warm area decoupling is found by observations of four years of surface remote sensing data from the ARM (Atmospheric Radiation Measurement) Cloud and Radiation Testbed site (Del Genio and Wolf, 2000). In an effort to explain the negative dependency of cloud optical thickness on surface temperature, they found that the boundary layers are different for cold and warm surface temperatures: stratified and convective boundary layers are associated with cold temperatures and mixed or decoupled boundary layers are associated with warm temperatures. Detailed analyses of boundary layer conditions show that while the decoupling of boundary layer is responsible for decreasing of cloud liquid water and thinning of the

Table I. Percentage of cloud liquid water sensitivity for different ranges

	$\delta=\Delta LWP/\Delta N_c < 0$				$\delta \approx 0$	$\delta=\Delta LWP/\Delta N_c > 0$					
	$\delta < -35$	$-35 < \delta$	$-25 < \delta$	$-15 < \delta$	$-5 < \delta$	$5 < \delta$	$15 < \delta$	$25 < \delta$	$35 < \delta$	$45 < \delta$	$95 < \delta$
		< -25	< -15	< -5	< 5	< 15	< 25	< 35	< 45	< 95	
Jan	1.07	1.98	8.93	27.3	40.9	9.69	3.76	2.12	1.49	1.24	1.49
	39.3				40.9	19.8					
Apr	1.89	1.84	6.15	20.8	38.9	11.4	5.97	3.77	2.99	2.52	3.77
	30.7				38.9	30.4					
Jul	1.31	2.85	9.55	22.6	37.1	8.72	5.04	3.31	2.52	2.60	4.46
	36.3				37.1	26.6					
Oct	0.73	1.28	5.11	19.6	44.9	11.8	7.77	4.26	2.23	1.28	1.03
	26.7				44.9	28.4					

cloud layer, it is not related to surface temperature (Del Genio and Wolf, 2000). In other words, warmer surface temperature alone is not the cause of the

decoupling of the boundary layer and the decreasing of cloud liquid water path; other factors must play a role in this process. The coincidence of negative liquid water

Table II. Relative liquid water sensitivity, β , and γ values in relation $r_c \sim N_c^\gamma$

	$\beta=\Delta \ln(LWP)/\Delta \ln(N_c) < 0$				$\beta \approx 0$	$\beta=\Delta \ln(LWP)/\Delta \ln(N_c) > 0$			
	$\beta < -70\%$	$-70\% < \beta$	$-50\% < \beta$	$-30\% < \beta$	$-10\% < \beta < 10\%$	$10\% < \beta$	$30\% < \beta$	$50\% < \beta$	$\beta > 70\%$
		$< -50\%$	$< -30\%$	$< -10\%$		$< 30\%$	$< 50\%$	$< 70\%$	
	$\gamma < -0.57$	$-0.57 < \gamma$	$-0.50 < \gamma$	$-0.43 < \gamma$	$-0.37 < \gamma$	$-0.30 < \gamma$	$-0.23 < \gamma$	$-0.17 < \gamma$	$-0.10 < \gamma$
		-0.50	-0.43	-0.37	-0.30	-0.23	-0.17	-0.10	
Jan	0.95	4.24	14.3	26.7	31.8	17.2	3.76	0.97	0.08
	46.2				31.8	22.0			
Apr	1.36	4.15	11.2	20.0	30.0	23.8	7.88	1.36	0.21
	36.7				30.0	33.3			
Jul	1.84	5.77	12.4	23.2	27.8	20.4	7.23	1.39	0.08
	43.2				27.8	29.1			
Oct	0.37	1.49	7.45	24.4	38.3	23.1	4.40	0.46	0.09
	33.7				38.3	28.0			

sensitivity in warmer seasons shown in the Figure 1 suggests a possible role for cloud microphysics. That is, increased droplet number concentration leads to decreases of droplet size (which is a global phenomena as will be shown later), hence to enhanced cloud base cooling due to evaporation and to reduced water supply from surface due to a weakened coupling between clouds and boundary layer.

Figure 2 shows histograms of the percentage of clouds for each liquid water sensitivity category with its values listed in Table 1. On an annual average, cloud liquid water sensitivities are negative about one third of the time and positive about a quarter of the time; these percentages vary somewhat with season.

4.2 Relative liquid water sensitivity

Figure 3 is a near-global survey of the relative liquid water sensitivity. It is apparent that, unlike the near-neutral absolute liquid water sensitivities, the relative liquid water sensitivities are mostly negative over land, which means that the relative change in liquid water path is notably related to the relative changes in column droplet number concentration even though the absolute changes are small. The mean and standard deviations for the relative liquid water sensitivity are: -0.098 ± 0.26 , -0.040 ± 0.29 , -0.077 ± 0.30 , and $.029 \pm 0.22$ for January, April, July and October 1987, respectively.

Figure 4 show histograms of the percentage of clouds for each relative liquid water sensitivity category with its values listed in the Table 2. On an annual average, the relative liquid water sensitivities are negative about 40% of the times, while they are positive about 28% of the times, these percentages

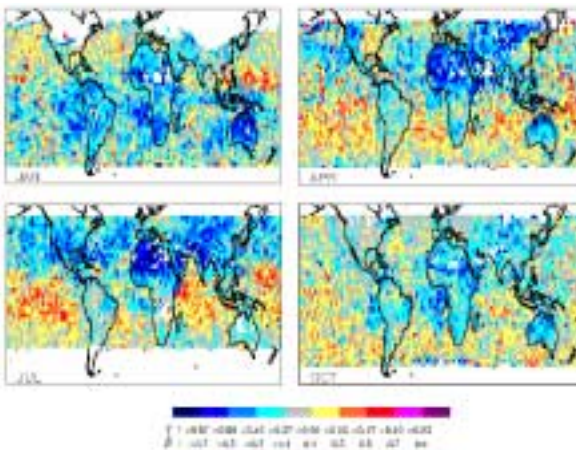


Figure 3: Relative liquid water sensitivity (β) and power γ in the relation $r_c \sim N_c^\gamma$ of water clouds for January, April, July and October 1987.

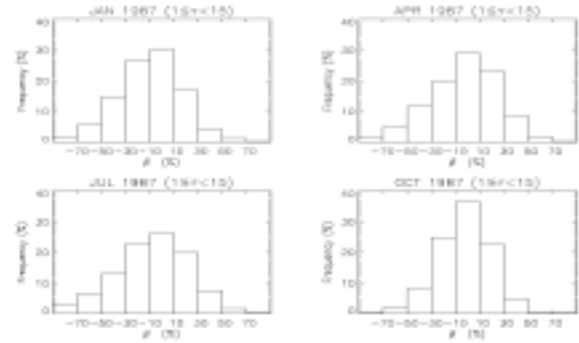


Figure 4: Histogram of the Relative liquid water sensitivity (β) of water clouds for January, April, July and October 1987.

vary somewhat with season.

Figures 3 and 4 reveal that the effective droplet radius and column droplet number concentration are always negatively correlated, suggesting that enhanced droplet number concentration always leads to decreased droplet size, although to different degrees. Many field observations find that a $(-1/3)$ power law is valid for relations between droplet radius and *volume* number concentrations but it was also noticed that variations in cloud layer thickness couldn't be neglected (e.g., Durkee et al., 2000; Ackerman et al., 2000). Our results show that in about one third of the cases the minus one third power law ($-0.37 < \gamma < -0.30$) is valid even for droplet radius and *column* number concentrations, which means that cloud layer thickness variations do not seem dominant.

5. Discussions and Conclusions

The response of cloud liquid water path to column droplet number concentration changes is an important part in estimating the aerosol indirect effect. In GCMs cloud liquid water path has been parameterized either as constant (Twomey Effect) or increasing with increasing droplet number concentrations due to suppression of drizzle (Albrecht Effect). Although model studies and field observations suggest that there may be another response, i.e., cloud liquid water content may be decreased with increasing droplet number concentrations, the relative frequency of this behavior has been unknown. This study examines the cloud responses (for clouds with top temperature > 273 K and optical thickness $1 \leq \tau < 15$) by retrieving the liquid water sensitivity on a near-global scale using satellite data and finds that more than in one third of the cases, the liquid water sensitivities are negative, i.e., cloud liquid water path decreases with increasing column number concentrations. Another finding of

this study is that although cloud droplet sizes always decrease with enhanced column droplet number concentrations as expected, for a majority of the cases, the quantitative relation between these r_e and N_c does not suggest an invariant liquid water path during aerosol-cloud interactions.

Regional and seasonal variations of the liquid water sensitivity show that most negative values are in the “warm zone” or summer hemisphere. This can be explained by the findings that the boundary layer is different in warm season from that in cold season at the ARM Southern Great Plains site: well-mixed or decoupled boundary layers in summer and well-stratified boundary layers in winter (Del Genio and Wolf, 2000). They also found that the decoupled boundary layer is strongly associated with a decreased liquid water path but decoupling is not dependent on surface temperature. Combined with their findings, our results suggest that the increased droplet number concentration leads to decreased droplet size and enhanced evaporation just below cloud base, which causes the boundary layer decoupling in warm zones, consistent with simulations of model studies (Ackerman et al., 1995).

We note that the pattern of retrieved liquid water sensitivity may include contributions from clouds formed in different air masses, which is especially true for areas close to coastlines. For example, maritime clouds with small droplet number concentration and continental clouds with large droplet number concentration are often both found in certain coast regions (e.g., Minnis et al., 1992; Twohy et al., 1995). Nevertheless, the negative liquid water sensitivity found in vast areas, including the remote ocean areas and relatively clean southern hemisphere, suggests that enhanced droplet number concentration plays an important role in inducing the decoupling of the boundary layer, reducing water vapor supply from the surface and desiccating cloud liquid water.

We also note that the results of this study should not be regarded as “before and after” aerosol-cloud interactions for individual clouds, instead, the results are statistical in nature. This should not be a problem when used for comparison with GCM results because cloud properties predicted by GCMs are also statistical in nature – they are not specific predictions for individual clouds in a weather system.

The results presented here are limited because they are for daytime-only, in fact afternoon-only, so that the aerosol-related changes in the clouds that we observe may not be true of the morning or nighttime changes. Although the day-time part of the cloud changes is most relevant to the albedo effect, we may not truly understand what is going on with marine boundary layer clouds and aerosol effects on them until we have comprehensive observations covering the whole

diurnal cycle, as well as all synoptic and seasonal variations. In addition, we are only able to correlate observed systematic changes in cloud properties, not actually observe their variation in time; hence, to confirm hypotheses of cause-and-effect will require supplementary in situ and ground-based measurements that actually resolve the cloud changes. However, the value of these results is to show that these relationships are not constant but dynamic in character, varying with meteorological regime.

Acknowledgments. This research is supported by NASA grants NAG5-7702, NCC8-200 and NAS1-98131.

6. References

- Ackerman, A. S., O. B. Toon, and P. V. Hobbs, 1993: Dissipation of marine stratiform clouds and collapse of the marine boundary layer due to the depletion of cloud condensation nuclei by clouds. *Science*, **262**, 226-229.
- Ackerman, A. S., O. B. Toon, and P. V. Hobbs, 1995: Numerical modeling of ship tracks produced by injections of cloud condensation nuclei into marine stratiform clouds. *J. Geophys. Res.*, **100**, 7121-7133.
- Ackerman, A. S., O. B. Toon, J. P. Taylor, D. W. Johnson, P. V. Hobbs, and R. J. Ferek, 2000: Effects of Aerosols on Cloud Albedo: Evaluation of Twomey’s Parameterization of Cloud Susceptibility Using Measurements of Ship Tracks. *J. Atmos. Sci.*, **57**, 2684-2695.
- Albrecht, B. A., 1989: Aerosols, cloud microphysics and fractional cloudiness. *Science*, **245**, 1227-1230.
- Alkezweeny, A. J., D. A. Burrows, and C. A. Grainger, 1993: Measurements of cloud droplet-size distributions in polluted and unpolluted stratiform clouds. *J. Appl. Meteor.*, **32**, 106-115.
- Beheng, K. D., 1994: A parameterization of warm cloud microphysical conversion processes, *Atmos. Res.*, **33**, 193-206.
- Boucher, O., and U. Lohmann, 1995: The sulfate-CCN-cloud albedo effect: a sensitivity study with two general circulation models. *Tellus*, **47B**, 281-300.
- Coakley, J. A. Jr., P. A. Durkee, K. Nielsen, J. P. Taylor, S. Platnick, B. A. Albrecht, D. Babb, F.-L. Chang, W. R. Tahnk, C. S. Bretherton, and P. V. Hobbs: 2000: The Appearance and Disappearance of Ship Tracks on Large Spatial Scales. *J. Atmos. Sci.*, **57**, 2765-2778.
- Del Genio, A. D., M. S. Yao, W. Kovari, and K. K. W. Lo, 1996: A prognostic cloud water parameterization for global climate models. *J. Climate*, **9**, 270-304.
- Del Genio, A. D., and A. B. Wolf, 2000: The temperature dependence of the liquid water path of low clouds

- in the southern great plains. *J. Climate*, **13**, 3465-3483.
- Durkee, P. A., K. J. Noone, R. J. Ferek, D. W. Johnson, J. P. Taylor, T. J. Garrett, P. V. Hobbs, J. G. Hudson, C. S. Bretherton, G. Innis, G. M. Frick, W. A. Hoppel, C. D. O'Dowd, L. M. Russell, R. Gasparovic, K. E. Nielsen, S. A. Tessmer, E. Ostrom, S. R. Osborne, R. C. Flagan, J. H. Seinfeld, and H. Rand, 2000: The Impact of Ship-Produced Aerosols on the Microstructure and Albedo of Warm Marine Stratocumulus Clouds: A Test of MAST Hypotheses Ii and Iii. *J. Atmos. Sci.*, **57**, 2554-2569.
- Eagan, R. C., P. V. Hobbs and L. F. Radke, 1974: Measurements of CCN and cloud droplet size distribution in the vicinity of forest fires. *J. Appl. Meteor.*, **13**, 553-537.
- Ferek, R. J., T. Garrett, P. Hobbs, S. Strader, D. Johnson, J. P. Taylor, K. Nielsen, A. S. Ackerman, Y. Kogan, Q. Liu, B. A. Albrecht, D. Babb, 2000: Drizzle suppression in ship tracks. *J. Atmos. Sci.*, **26**, 2707-2728.
- Fitzgerald, J. W., and P. A. Spyers-Duran, 1973: Changes in cloud nucleus concentration and cloud droplet size distribution associated with pollution from St. Louis. *J. Appl. Meteor.*, **12**, 511-516.
- Ghan, S. J., L. R. Leung, R. C. Easter, and H. A. Razzak, 1997: Prediction of cloud droplet number in a general circulation model. *J. Geophys. Res.*, **102**, 21777-21794.
- Ghan, S., R. C. Easter, E. Chapman, H. Abdul-Razzak, Y. Zhang, R. Leung, H. Laulainen, R. Saylor, and R. Zaveri, 2000: A physically-based estimate of radiative forcing by anthropogenic sulfate aerosol. *J. Geophys. Res.*, **106**, 5279-5294.
- Greenwald, T. J., G. L. Stephens, S. A. Christopher, and T. H. Vonder Haar, 1995: Observations of the global characteristics and regional radiative effects of marine cloud liquid water. *J. Climate*, **8**, 2928-2946.
- Greenwald, T. J., S. A. Christopher, and J. Chou, 1997: SSM/I and GOES-8 imager comparisons of cloud liquid water path over water: Assessment of sub-field of view effects in microwave retrievals. *J. Geophys. Res.*, **102**, 19585-19596.
- Griggs, M., 1983: Satellite measurements of tropospheric aerosols. *Advances in Space Research*, **2**, 109-118.
- Han, Q., W. B. Rossow, and A. A. Lacis, 1994: Near-global survey of effective droplet radii in liquid water clouds using ISCCP data. *J. Climate*, **7**, 465-497.
- Han, Q., W. Rossow, R. Welch, A. White, and J. Chou, 1995: Validation of satellite retrievals of cloud microphysics and liquid water path using observations from FIRE. *J. Atmos. Sci.*, **52**, 4183-4195.
- Han, Q. Y., W. B. Rossow, J. Chou, and R. M. Welch, 1998a: Global survey of the relationship of cloud albedo and liquid water path with droplet size using ISCCP. *J. Climate*, **11**, 1516-1528.
- Han, Q. Y., W. B. Rossow, J. Chou, and R. M. Welch, 1998b: Global Variation of Cloud Effective Droplet Concentration of Low-level Clouds. *Geophys. Res. Letts.* **1419-1422**.
- Han, Q. Y., W. B. Rossow, J. Chou, and R. M. Welch, 2000: Near-global survey of cloud column susceptibility using ISCCP data. *Geophys. Res. Letts.* **27**, 3221-3224.
- Hansen, J., M. Sato, A. Lacis, and R. Ruedy, 1997b: The missing climate forcing. *Phil. Trans. R. Soc. Lond.*, **B 352**, 231-240.
- Hobbs, P. V., L. F. Radke, and S. E. Shumway, 1970: Cloud condensation nuclei from industrial sources and their apparent influence on precipitation in Washington State. *J. Atmos. Sci.*, **27**, 81-89.
- Hudson, J. G., and G. Svensson, 1995: Cloud microphysical relationships in California marine stratus. *J. Appl. Meteor.*, **34**, 2655-2666.
- Hudson, J. G., T. J. Garrett, P. V. Hobbs, S. R. Strader, Y. Xie, and S. S. Yum, 2000: Cloud condensation nuclei and ship tracks. *J. Atmos. Sci.*, **57**, 2696-2706.
- Intergovernmental Panel on Climate Change, 1996: *Climate Change 1995: The Science of Climate Change*, J. T. Houghton, L. G. Meira Filho, B. A. Callander, N. Harris, A. Katenberg, and K. Maskell (eds), Cambridge Univ. Press, Cambridge, 572pp.
- Jones, A., D. L. Roberts, and A. Slingo, 1994: A climate model study of indirect radiative forcing by anthropogenic sulphate aerosols. *Nature*, **370**, 450-453.
- Jones, A., and Slingo, A., 1996: Predicting cloud-droplet effective radius and indirect sulphate aerosol forcing using a general circulation model. *Quart. J. Roy. Meteor. Soc.*, **122**, 1573-1595.
- Jones, A., D. L. Roberts, and M. J. Woodage, 1999: The indirect effect of anthropogenic sulphate aerosol simulated using a climate model with an interactive sulphur cycle. [*Quart. J. Roy. Meteorol. Soc.*, submitted]
- Lacis, A. A., and V. Oinas, 1991: A description of the correlated k-distribution method for modeling non-grey gaseous absorption, thermal emission, and multiple scattering in vertically inhomogeneous atmospheres. *J. Geophys. Res.* **96**, 9027-9063.
- Lin, B., and W. B. Rossow, 1994: Observations of cloud liquid water path over oceans: Optical and microwave remote sensing methods. *J. Geophys. Res.*, **99**, 20907-20927.

- Lin, B., and W. B. Rossow, 1996: Seasonal variation of liquid and ice water path in nonprecipitating clouds over oceans. *J. Climate*, **9**, 2890-2902.
- Lohmann, U., and J. Feichter, 1997: Impact of sulfate aerosols on albedo and lifetime of clouds, A sensitivity study with the ECHAM4 GCM. *J. Geophys. Res.*, **102**, 13685-13700.
- Lohmann, U., and J. Feichter, C. C. Chuang, and J. E. Penner, 1999: Predicting the number of cloud droplets in the ECHAM GCM, *J. Geophys. Res.*, **104**, 9169-9198.
- Martin, G. M., D. W. Johnson, and A. Spice, 1994: The measurement and parameterization of effective radius of droplets in warm stratocumulus clouds. *J. Atmos. Sci.*, **51**, 1823-1842.
- Menon, S., A. Del Genio, G. Koch, and G. Tselioudis, 2002: GCM simulations of the aerosol indirect effect: Sensitivity to cloud parameterization and aerosol burden. *J. Atmos. Sci.*, *this issue*.
- Minnis, P., P. W. Heck, D. F. Young, C. W. Fairall, and J. B. Snider, 1992: Stratocumulus cloud properties derived from simultaneous satellite and island-based instrumentation during FIRE. *J. Appl. Meteor.*, **31**, 317-339.
- Nakajima, T., M. D. King, and J. D. Spinhirne, 1991: Determination of the optical thickness and effective particle radius of clouds from reflected solar radiation measurements. Part II: Marine stratocumulus observations. *J. Atmos. Sci.*, **48**, 728-750.
- Pincus, R., and M. B. Baker, 1994: Effect of precipitation on the albedo susceptibility of clouds in the marine boundary layer. *Nature*, **372**, 250-252.
- Platnick, S., and S. Twomey, 1994: Determining the susceptibility of cloud albedo to changes in droplet concentration with the Advanced Very High Resolution Radiometer. *J. Appl. Meteor.*, **33**, 334-347.
- Platnick, S., P. A. Durkee, K. Nielsen, J. P. Taylor, S. C. Tsay, M. King, R. J. Ferek, and P. V. Hobbs, 2000: The role of background microphysics in the radiative formation of ship tracks. *J. Atmos. Sci.*, **57**, 2607-2624.
- Radke, L. F., and J. A. Coakley, Jr., M. D. King, 1989: Direct and remote sensing observations of the effects of ships on clouds. *Science*, **246**, 1146-1149.
- Rosenfeld, D., 1999: TRMM observed first direct evidence of smoke from forest fires inhibiting rainfall. *Geophys. Res. Lett.* **26**, 3105-3108.
- Rossow, W. B., L. C. Garder and A. A. Lacis, 1989: Global, seasonal cloud variations from satellite radiance measurements. Part I: Sensitivity of analysis. *J. Climate* **2**, 419-458.
- Rotstayn, L. D., 1999: Indirect forcing by anthropogenic aerosols: A global climate model calculation of the effective-radius and cloud-lifetime effects, *J. Geophys. Res.*, **104**, 9369-9380.
- Twohy, C. H., P. A. Durkee, R. J. Huebert, and R. J. Charlson, 1995: Effects of aerosol particles on the microphysics of coastal stratiform clouds. *J. Climate*, **8**, 773-783.
- Twomey, S., 1974: Pollution and the planetary albedo. *Atmos. Environ.*, **8**, 1251-1256.
- Twomey, S., 1991: Aerosols, clouds and radiation. *Atmospheric Environment*, **25A**, 2435-2442.
- Twomey, S., 1993: Radiative properties of clouds. In *Aerosol Effects on Climate*. S. G. Jennings, Editor, The University of Tuscon Press, p275-298.
- Wang, J., W. B. Rossow, and Y. Zhang, 2000: Cloud Vertical Structure and Its Variations from a 20-Yr Global Rawinsonde Dataset. *J. Climate*, **13**, 3041-3056.